A Time-Domain Full-Wave Extraction Method of Frequency-Dependent Equivalent Circuit Parameters of Multiconductor Interconnection Lines

Jin Zhao and Zheng-Fan Li

***Abstract*—A time-domain full-wave method for the extraction of frequency-dependent equivalent circuit parameters of multiconductor interconnection lines is presented in this paper. The circuit parameters extracted by this method can be inserted into circuit simulation software to investigate time-domain responses of high-speed IC system with multiconductor interconnects. Because the definitions of the voltage and the current are not unique in full-wave analysis, transformation among circuit parameters according to different definitions of the voltage and current is also presented. The method is based on the finite-difference time-domain (FDTD) method, and the reliability of this method is illustrated by its application to representative problems.**

I. Introduction

ELECTROMAGNETIC modeling plays an important role in the design of electronic packages. As the speed or frequency of high-performance package increases, much effort has been placed on the performance of the interconnects and package structures driven by very short pulse signals. The increasing interconnection densities combined with high-speed circuit cells have exacerbated the problems such as time delay, signal degradation, clock skew, and crosstalk in electronic packages. Thus, accurate modeling of these interconnection structures is necessary to ensure the correct simulation of the electrical performance in the design stage.

In the past years, many methods for modeling multiconductor interconnection lines have been based on quasi-TEM assumption, and the frequency dependency of the distributed circuit parameters has been neglected. A variety of methods for the extraction of the quasi-TEM parameters are available, such as the method of moments [1], the method of lines [2], the method of moments combined with spectral-domain Green's function [3], etc. When the signal speed increases, high-frequency components of the signal spectrum must be taken into account. High-frequency effects such as the appearance of longitudinal field components are no longer negligible. The full-wave nature of the interconnects becomes important. A frequency-dependent circuit modeling based upon full-wave analysis is necessary.

Several frequency-domain methods based upon the full-wave analysis are available for the extraction of the equivalent circuit parameters of the interconnection lines [4], [5]. Most of them are concerned with the extraction of modal parameters such as mode-phase velocities, mode-characteristic impedances, etc. Only a few of them provide computation results of the inductance and capacitance matrices for multiconductor interconnects [6], [7]. Recently, research work was done in time domain by the finite-difference time-domain (FDTD) method [8], [9]. However, the focal point was still on the field distribution or scattering parameters, not on the circuit parameters that are directly needed by the circuit simulation software.

This paper presents a time-domain method for extracting the frequency-dependent $[L]$ and $[C]$ matrices of multiconductor interconnection lines. The method is based upon the FDTD method [10], which has recently been used by many authors in packaging applications [11]–[13]. The reason for using $[L]$ and $[C]$ matrices as circuit parameters is that they are widely used in circuit simulation. On the other hand, the multiconductor structure can also be treated as multiconductor transmission lines, which are widely used in some microwave passive components such as directional couplers, filters, bridges, etc. So, the proposed method can also be used to extract the equivalent circuit parameters of multiconductor transmission lines for microwave integrated circuits (MIC's).

In this paper, the equivalence between a full-wave solution of multiconductor lines by the FDTD method and a corresponding circuit modeling solution of the lines is first described. Then, the extraction procedure of $[L]$ and $[C]$ matrices from the data obtained by the FDTD method is given. To show the reliability of this method, the results are verified by comparison with other methods and by the circuit simulation. After a short discussion of the definition of characteristic impedances for microstrip transmission lines, the transformation among different $[L], [C]$ results corresponding to different definitions of the voltage and current is given. The limitation of applying the distributed circuit model with frequency-dependent parameters for multiconductor interconnection lines in very large scale integration (VLSI) or multiconductor transmission lines in MIC is discussed in the end.

II. Parameter Extraction

The structure of N-conductor interconnection lines is shown in Fig. 1. The lines can be embedded in inhomogeneous dielectric media. According to electromagnetic field theory, when the frequency is not very high the structure can be

Manuscript received August 22, 1995; revised September 23, 1996. This work was supported by the National Natural Science Foundation of China.

The authors are with the Department of Electronic Engineering, Shanghai Jiao Tong University, Shanghai 200052, China.

Publisher Item Identifier S 0018-9480(97)00262-7.

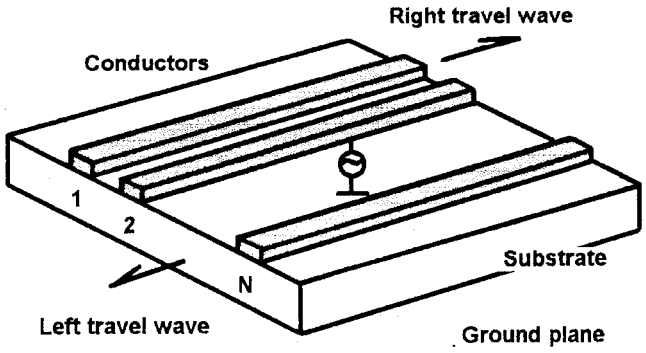

Fig. 1. The structure of multiconductor interconnection line.

considered as a guided-wave system and can be described by the distributed circuit parameters of transmission lines. The voltage and current on the transmission lines satisfy the telegrapher's equations in frequency domain [14]

$$\frac{d}{dz}[V(z,\omega)] = -[Z(\omega)][I(z,\omega)]$$
$$\frac{d}{dz}[I(z,\omega)] = -[Y(\omega)][V(z,\omega)] \tag{1}$$

where $[Z(\omega)] = [R(\omega)] + j\omega[L(\omega)], [Y(\omega)] = [G(\omega)] + j\omega[C(\omega)]$. The $[V(z,\omega)]$ and $[I(z,\omega)]$ are the voltage and current vectors with variable z and ω in frequency domain. $[R(\omega)], [G(\omega)], [L(\omega)]$ and $[C(\omega)]$ are frequency-dependent matrices of equivalent circuit distributed parameters. Let $[R(\omega)] = 0$ and $[G(\omega)] = 0$ for simplicity, (1) then becomes

$$\frac{d}{dz}[V(z,\omega)] = -j\omega[L(\omega)][I(z,\omega)]$$
$$\frac{d}{dz}[I(z,\omega)] = -j\omega[C(\omega)][V(z,\omega)]. \tag{2}$$

From (2), one can see that the voltage $[V(z,\omega)]$ and current $[I(z,\omega)]$ along transmission lines can be calculated after the capacitance $[C(\omega)]$, inductance $[L(\omega)]$, and boundary conditions are given. The waveform of the voltage and current along the transmission lines in time domain can be obtained from inverse Fourier transformation.

The FDTD method is used to simulate the electromagnetic fields propagating in the structure. The fields' distribution at any position and time within the calculation region can be recorded. The corresponding voltage, current, and transmission power can also be calculated by their definitions. The crux relies in how to extract the equivalent distributed circuit parameters of the lines from the voltage and current data.

For the structure of N-conductor interconnection lines shown in Fig. 1, N orthogonal excitations are needed. Each time only one conductor is excited while others are not. After sampling the voltage and current data along the lines for N times of excitation, (2) becomes

$$\frac{d}{dz}[[V(z,\omega)]_1 \quad [V(z,\omega)]_2 \quad \cdots \quad [V(z,\omega)]_N]$$
$$= -j\omega[L(\omega)][[I(z,\omega)]_1 \quad [I(z,\omega)]_2 \quad \cdots \quad [I(z,\omega)]_N]$$
$$\frac{d}{dz}[[I(z,\omega)]_1 \quad [I(z,\omega)]_2 \quad \cdots \quad [I(z,\omega)]_N]$$
$$= -j\omega[C(\omega)][[V(z,\omega)]_1 \quad [V(z,\omega)]_2 \quad \cdots \quad [V(z,\omega)]_N]. \tag{3}$$

After defining the matrix $[[V(z,\omega)]]$ and $[[I(z,\omega)]]$ as

$$[[V(z,\omega)]] = [[V(z,\omega)]_1 \quad [V(z,\omega)]_2 \quad \cdots \quad [V(z,\omega)]_N]$$
$$[[I(z,\omega)]] = [[I(z,\omega)]_1 \quad [I(z,\omega)]_2 \quad \cdots \quad [I(z,\omega)]_N] \tag{4}$$

the frequency-dependent inductance $[L(\omega)]$ and capacitance $[C(\omega)]$ matrices can be obtained by

$$[L(\omega)] = -\frac{1}{\omega}\,\mathrm{Im}\left(\frac{d}{dz}[[V(z,\omega)]][[I(z,\omega)]]^{-1}\right)$$
$$[C(\omega)] = -\frac{1}{\omega}\,\mathrm{Im}\left(\frac{d}{dz}[[I(z,\omega)]][[V(z,\omega)]]^{-1}\right) \tag{5}$$

where "Im" means imaginary part of a complex number. The derivatives $[[V(z,\omega)]]'$ and $[[I(z,\omega)]]'$ with respect to z along the lines are accomplished by a numerical method such as central differencing. One can also obtain the characteristic impedances from these parameters, as well as the effective dielectric constants that determine the phase velocities along the lines (see Appendix).

The electromagnetic fields calculated by the FDTD algorithm were considered as a simulation of electromagnetic fields within the calculation region of the multiconductor lines. The voltage and current are defined as

$$I = \oint_c \overline{H}\cdot\overline{dl} \tag{6}$$

$$V = \int_h^0 \overline{E}\cdot\overline{dl} \tag{7}$$

where c is the transverse contour of a conductor and h is the distance between a conductor and the ground plane.

The extraction procedure begins with a simulation of electromagnetic fields by the FDTD method. Superabsorption boundary condition [15] is used in this work. The excitation source is chosen to be a Gaussian pulse. The excitation plane is put into the calculation region, which equals to exciting the electromagnetic field in the middle of the transmission lines (see Fig. 2). To avoid the influence of high-order modes and reflection waves from the imperfect absorbing boundary, the sample points are chosen carefully in the middle of the excitation plane and the absorbing end where the transmission modes have already formed. The sample period is also chosen carefully so that the incident wave can be recorded completely and the reflection waves from both sides have not come back yet.

III. Reliability Verification

The reliability of the above extraction is verified by the circuit simulation. Considering an N-conductor transmission lines' structure with circuit parameters $[C(\omega)]$ and $[L(\omega)]$, which have just been extracted, suppose line one is driven by a Gaussian pulse-voltage source at the middle of the line. The lines are supposed to be infinitely long so there are no end loads and no reflections on lines. Because of the symmetric property, a magnetic wall is set at the position of the excitation plane. The boundary condition of the excitation position is

$$v_1(t) = g(t)$$
$$i_m(t) = 0, \qquad (m = 2, \cdots, N) \tag{8}$$

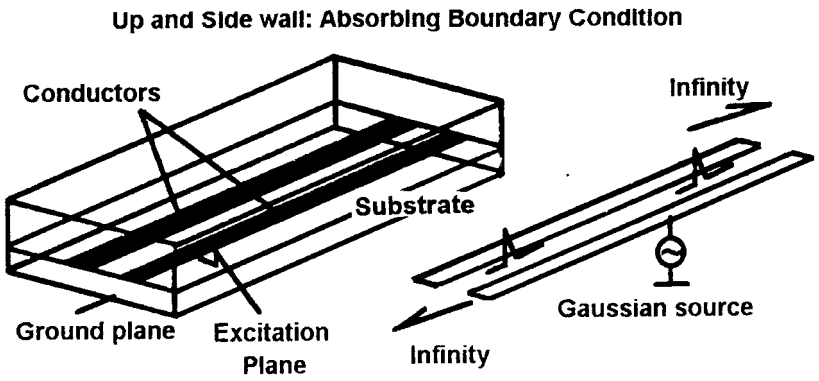

Fig. 2. Electromagnetic fields of multiconductor structure under excitation and its equivalent transmission line.

where $g(t)$ is the Gaussian pulse source. The telegrapher's equations are solved in frequency domain after taking fast Fourier transform (FFT) on the Gaussian pulse.

According to the theory of transmission line or microwave network theory, the voltage and current on transmission lines can be expressed by eigenmodes in frequency domain:

$$\begin{bmatrix} V_1 \\ V_2 \\ \vdots \\ V_N \end{bmatrix} = \begin{bmatrix} e_{11} & e_{21} & \cdots & e_{N1} \\ e_{12} & e_{22} & \cdots & e_{N2} \\ \vdots & \vdots & \ddots & \vdots \\ e_{1N} & e_{2N} & \cdots & e_{NN} \end{bmatrix} \operatorname{diag}(e^{-\gamma_m z}) \begin{bmatrix} a_1 \\ a_2 \\ \vdots \\ a_N \end{bmatrix}$$

$$\begin{bmatrix} I_1 \\ I_2 \\ \vdots \\ I_N \end{bmatrix} = \begin{bmatrix} e_{11} & e_{21} & \cdots & e_{N1} \\ e_{12} & e_{22} & \cdots & e_{N2} \\ \vdots & \vdots & \ddots & \vdots \\ e_{1N} & e_{2N} & \cdots & e_{NN} \end{bmatrix} \operatorname{diag}\left(\frac{1}{Z_{0m}}\right) \cdot \operatorname{diag}(e^{-\gamma_m z}) \begin{bmatrix} a_1 \\ a_2 \\ \vdots \\ a_N \end{bmatrix}, \qquad (m = 1, \cdots, N) \quad (9)$$

where V_i and I_i are the voltage and current on the ith conductor, e_{ij} is the component of mode i on conductor j, matrix $[e_{ij}]$ is a unique eigenmode matrix, γ_m and Z_{0m} are the propagation constant and the characteristic impedance of the mth mode, and a_i is the mode coefficient. The reflection wave has been neglected because of the infinite length of the lines. This satisfies the condition in the field simulation with the FDTD method.

At $z = 0$, the following equation can be derived from (9):

$$\begin{bmatrix} V_1(0) \\ V_2(0) \\ \vdots \\ V_N(0) \end{bmatrix} = [e_{ij}] \operatorname{diag}(Z_{cm}) [e_{ij}]^{-1} \begin{bmatrix} I_1(0) \\ I_2(0) \\ \vdots \\ I_N(0) \end{bmatrix}, \qquad (m = 1, \cdots, N). \quad (10)$$

Define $[Q]$ as

$$[Q] = [e_{ij}] \operatorname{diag}(Z_{cm}) [e_{ij}]^{-1}, \qquad (m = 1, \cdots, N). \quad (11)$$

According to the boundary condition (8), the voltage on every line and the current on line one can be calculated:

$$V_m(0) = \frac{Q_{m1}}{Q_{11}} V_1(0)$$
$$I_1(0) = \frac{1}{Q_{11}} V_1(0), \qquad (m = 2, \cdots, N). \quad (12)$$

So, at position z the voltage and current vectors are

$$\begin{bmatrix} V_1(z) \\ V_2(z) \\ \vdots \\ V_N(z) \end{bmatrix} = [e_{ij}] \operatorname{diag}(e^{-\gamma_m z}) [e_{ij}]^{-1} \begin{bmatrix} V_1(0) \\ V_2(0) \\ \vdots \\ V_N(0) \end{bmatrix}$$

$$\begin{bmatrix} I_1(z) \\ I_2(z) \\ \vdots \\ I_N(z) \end{bmatrix} = [e_{ij}] \operatorname{diag}\left(\frac{1}{Z_{0m}}\right) \operatorname{diag}(e^{-\gamma_m z}) [e_{ij}]^{-1} \cdot \begin{bmatrix} V_1(0) \\ V_2(0) \\ \vdots \\ V_N(0) \end{bmatrix}, \qquad (m = 1, \cdots, N). \quad (13)$$

After that, the inverse fast Fourier transformation (IFFT) is taken to transform $[V(z, \omega)]$ and $[I(z, \omega)]$ back to time domain. The voltage waveform $[v(z, t)]$ and current waveform $[i(z, t)]$ along the lines can be obtained. By comparing that with the voltage waveform $[v(z, t)]$ and current waveform $[i(z, t)]$ recorded while running the FDTD algorithm, the verification of this method can be accomplished. The following example shows that the two results agree well with each other; it means that the method is reliable.

IV. Transformation Among the Parameters with Different V and I Definitions

It is generally agreed that for non-TEM structures such as microstrip lines the definition of characteristic impedance is not unique. Usually, there are three definitions of characteristic impedance [16]:

1) the voltage–current definition:

$$Z_0 = V/I \quad (14)$$

2) the power-voltage definition:

$$Z_0 = |V|^2/(2P) \quad (15)$$

3) the power-current definition:

$$Z_0 = 2P/|I|^2 \tag{16}$$

where I and V are defined by (6) and (7), respectively; P is the power transmitted in the structure.

When the frequency is not high, the three definitions are identical because the voltage and current have certain definitions and

$$P = VI \tag{17}$$

is valid. But as the frequency becomes higher, the above description is incorrect, and the three definitions of Z_0 lead to different values.

The above conclusion is also valid for the $[L(\omega)]$ and $[C(\omega)]$ matrices of the multiconductor lines. The voltage and current used for extraction by first definition is convenient to be obtained because only a few data of electromagnetic fields must be recorded. We will describe how to find the parameters with other definitions, for example, obtaining the transformation among them upon the concept of the power equivalence. Here, the transformation of the $[L(\omega)], [C(\omega)]$ matrices from the first definition into the third definition is presented.

When running the FDTD algorithm, the voltage $[v(z,t)]$, current $[i(z,t)]$, and transient power $p(z,t)$ could be calculated and recorded. $p(z,t)$ is defined by

$$p(z,t) = \iint \overline{E} \times \overline{H} \cdot d\overline{s}. \tag{18}$$

The following equation is used as power equal condition in this paper, which means the power transmitted by the actual physical system is equal to the equivalent circuit system at any time

$$\begin{aligned} p_{\text{actual system}}(z,t) &= p_{\text{equivalent circuit system}}(z,t) \\ &= [v_{\text{equivalent circuit system}}(z,t)^T \\ &\quad \cdot [i_{\text{equivalent circuit system}}(z,t)] \end{aligned} \tag{19}$$

where T means transposition.

It is well known that in microstrip-type structures, the current has its physical meaning, but the voltage does not and, here, the power $p(z,t)$ also has its physical meaning. What we want to do is to find out another voltage $[v_p(z,t)]$ that satisfies (19). The subscript p means referring to the power. Let

$$[v_p(z,t)] = \text{diag}\,(a_m(t))[v(z,t)], \qquad (m = 1, \cdots, N) \tag{20}$$

where $\alpha_m(t)$ is named as transformation factor.

A structure of two coupled transmission lines is used to show how it works. After running the FDTD program twice, total transferred power $p'(t), p''(t)$ can be obtained. Superscript "$'$" and "$''$" means for the first and second time. $i_1'(t), i_1''(t)$ and $i_2'(t), i_2''(t)$ are currents defined by (6). Subscript 1(2) means on conductor 1(2). $v_1'(t), v_1''(t)$ and $v_2'(t), v_2''(t)$ correspond to the voltages defined by (7). Rewrite (19), but with $v_p(t)$ defined by (20) instead of $v(t)$:

$$\begin{aligned} p'(t) &= \alpha_1(t)v_1'(t)i_1'(t) + \alpha_2(t)v_2'(t)i_2'(t) \\ p''(t) &= \alpha_1(t)v_1''(t)i_1''(t) + \alpha_2(t)v_2''(t)i_2''(t). \end{aligned} \tag{21}$$

By solving this equation, $\alpha_1(t), \alpha_2(t)$ can be obtained and one has

$$\begin{aligned} v_{p1}'(t) &= a_1(t)v_1'(t) \quad v_{p1}''(t) = a_1(t)v_1''(t) \\ v_{p2}'(t) &= a_2(t)v_2'(t) \quad v_{p2}''(t) = a_2(t)v_2''(t). \end{aligned} \tag{22}$$

Take Fourier transformation on (22)

$$\begin{aligned} V_{p1}'(\omega) &= \alpha_1(\omega) * V_1'(\omega) = \xi_1(\omega)V_1'(\omega) \\ V_{p2}'(\omega) &= \alpha_2(\omega) * V_2'(\omega) = \xi_2(\omega)V_2'(\omega) \\ V_{p1}''(\omega) &= \alpha_1(\omega) * V_1''(\omega) = \xi_1(\omega)V_1''(\omega) \\ V_{p2}''(\omega) &= \alpha_2(\omega) * V_2''(\omega) = \xi_2(\omega)V_2''(\omega) \end{aligned} \tag{23}$$

where $\xi_1(\omega)$ and $\xi_2(\omega)$ are transformation factors in frequency domain corresponding to $\alpha_1(t)$ and $\alpha_2(t)$ in time domain. Rewrite (23) as

$$[V_p(\omega)] = \text{diag}\,(\xi_m)[V(\omega)], \qquad (m = 1, \cdots, N). \tag{24}$$

Then, take the derivatives of $[V(z,\omega)]$ and $[I(z,\omega)]$

$$\frac{d}{dz}[V_p(\omega)] = \text{diag}\,(\xi_m)\frac{d}{dz}[V(\omega)], \qquad (m = 1, \cdots, N). \tag{25}$$

With (25) in (2), one has

$$\begin{aligned} &[L_p(\omega)] = \text{diag}\,(\xi_m)[L(\omega)] \quad \text{and} \\ &[C_p(\omega)] = [C(\omega)]\,\text{diag}\left(\frac{1}{\xi_m}\right), \quad (m = 1, \cdots, N). \end{aligned} \tag{26}$$

Define

$$T_p = \text{diag}\,(\xi_m), \qquad (m = 1, \cdots, N) \tag{27}$$

as a transformation matrix between different definitions of the voltage.

Finally, the role of the transformation factor is being shown. Still use two coupled lines as an example and have

$$\begin{aligned} p'(t) &= v_{1p}'(t)i_1'(t) + v_{2p}'(t)i_2'(t) \\ p''(t) &= v_{1p}''(t)i_i''(t) + v_{2p}''(t)i_2''(t). \end{aligned} \tag{28}$$

From (28) one can see that at any time there are four unknown voltages $(v_1', v_2', v_1'', v_2'')$ but with two equations. After introducing the transformation factor, there are only two unknown variables, so (28) can be solved with the help of (21).

The transformation factor represents the relationship between different definitions of the voltage. The relationship does not change with the extra excitation. The transformation factor is only decided by the properties of the structure. With the transformation factor, the computation of the power and current of the structure, the voltage of an equivalent system can be obtained. With the voltage and current, the equivalent circuit parameters can be extracted from the equivalent model.

V. Examples of Extraction and Its Verification

In this section, two practical structures will be considered. We will follow the procedure, which was proposed in Section II to extract the equivalent distributed circuit parameters, and then take circuit simulation proposed in Section III with the circuit parameters just extracted. The reliability of this method will be shown by comparing the voltage waveform

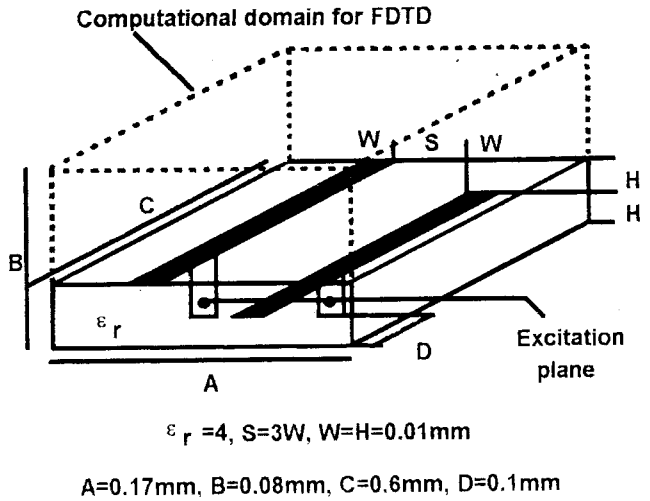

Fig. 3. Cross section of asymmetric coupled lines.

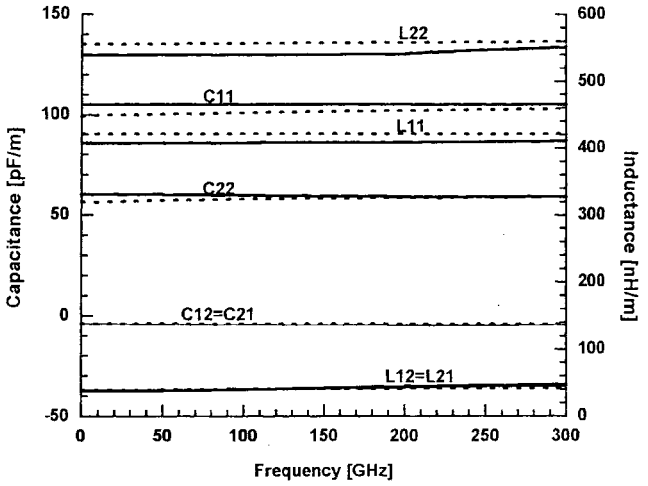

Fig. 4. The results of inductance and capacitance matrices of the asymmetric coupled lines shown in Fig. 3. Solid line: this method. Dashed line: method of [7].

generated by the circuit simulation and that recorded by running the FDTD algorithm. We will also show the distributed circuit parameters and wave-property parameters such as effective dielectric constants and characteristic impedances with different definitions.

The first example is an asymmetric coupled interconnection lines used in VLSI [7]. Fig. 3 gives the geometrical size of the structure and the parameters for the FDTD simulation. The number of grid is 85 × 40 × 300 with space $\Delta h = 2\times 10^{-6}$ m. Time interval Δt is 2.213×10^{-15} s. Run the FDTD algorithm with $NT = 2000$ time steps. The excitation source is a Gaussian pulse with $t_0 = 200\Delta t$ and $T = 40\Delta t$. The excitation plane is put into the box with 50 Δh.

Because Δt is too small, the Δf after FFT is too much larger to show the results. To have small Δf, the time points used for FFT must be very large, which will lead low efficiency of the FFT; most frequency points will be useless. In this paper, the following formula derived from the definition of Fourier transformation is used:

$$F(\omega) = \sum_{i=0}^{NT} f(i) e^{-j\omega(i\Delta t)} \Delta t \tag{29}$$

where $f(i)$ is the sample of the voltage or the current. The condition for (29) is that the pulse wave must pass the sample points completely when time reaches $NT\Delta t$. Here, Δf is 10 GHz.

Fig. 4 shows the $[C(\omega)]$ and $[L(\omega)]$ matrices extracted by this method. It has been shown that the performance of TEM mode or quasi-TEM mode keeps working well in a very wide frequency range. The results from our method are very close to that of [7] using the frequency-domain method.

The second example is a structure used in MIC [8] with symmetric two-coupled transmission lines. Fig. 5 shows the geometrical parameters of the structure. The space Δh is 5×10^{-5} m. Time interval Δt is 5×10^{-14} s with $NT = 1600$. $t_0 = 500\Delta t, T = 100\Delta t$.

Fig. 6 shows the waveform of the voltage and current defined by (6) and (7) at different positions along the coupled transmission lines recorded during a running FDTD algorithm.

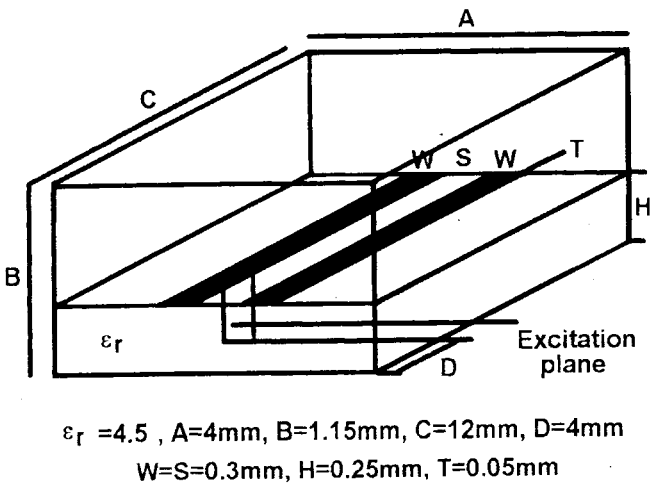

Fig. 5. Cross section of symmetric coupled lines. The perfectly conducting strips are 0.05 mm by 0.3 mm and separated by 0.3 mm. The dielectric slab is 0.25-mm thick and has a relative dielectric constant ε_r of 4.5.

One can see the distortion of the pulse along the excited line and the coupled quantity on the second line. The $[C(\omega)]$ and $[L(\omega)]$ extracted by this method as the functions of frequency are shown in Fig. 7. After voltage modification to keep the common power, the $[L(\omega)], [C(\omega)]$ matrices with third definition are also obtained. The curves are shown in the same figure to compare with that of the first definition. Figs. 8 and 9 show the effective dielectric constants and characteristic impedances of even and odd modes of the structures that derived from different distributed circuit parameters. From Figs. 8 and 9, one can see that the voltage transformation does not change the wave-propagation performance, but affects the characteristic impedances. When the frequency becomes lower, the transformation factor reaches one (see Fig. 10), meaning that the various definitions are common at lower frequency.

Finally, we verify the above results by the circuit simulation procedure proposed in Section IV and found that they agree well with each other (Fig. 6—dashed line). This means that

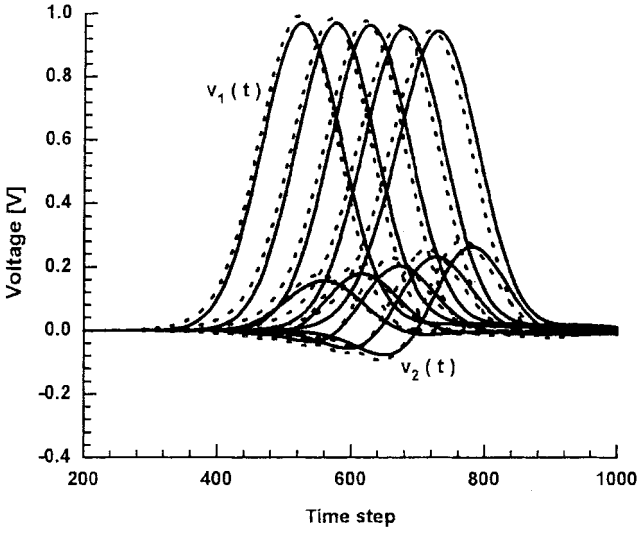

(a)

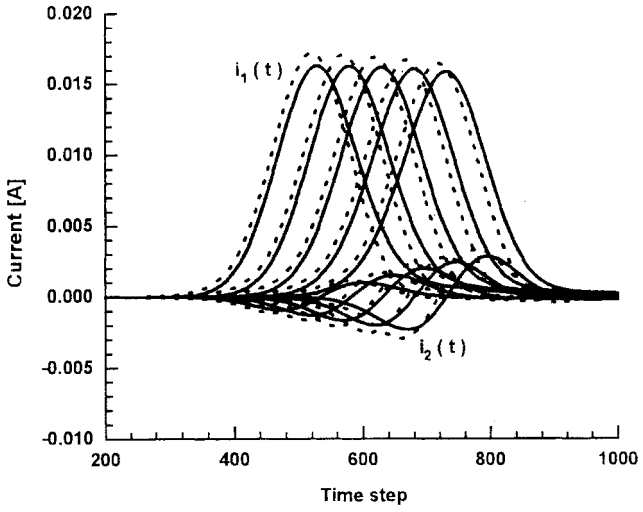

(b)

Fig. 6. Time variation of voltage and current waveform (on conductor 1, 2) at different positions (40, 60, 80, 100, 120 relative to the excitation point) along the direction of propagation. Solid line: recorded when running the FDTD algorithm. Dashed line: obtained by circuit simulation.

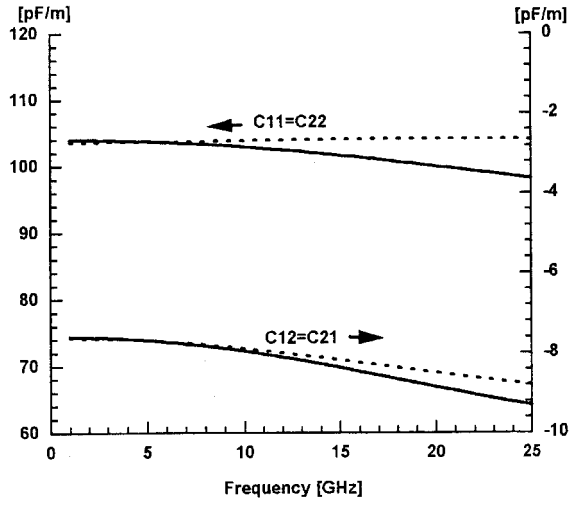

(a)

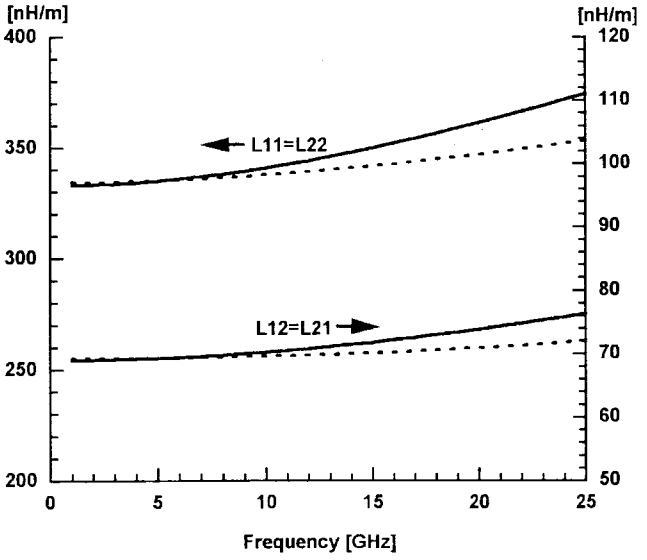

(b)

Fig. 7. Comparison of the circuit distributed parameters of the symmetric coupled lines shown in Fig. 5 before (dashed line) and after (solid line) voltage transformation.

the parameters extracted by this method are reliable for use in circuit simulation and analysis.

VI. Application Range of Traditional Circuit Modeling

As mentioned above, the FDTD method solves Maxwell's equations directly, so the field results generated by the FDTD method are considered as a real or true solution. After giving the definition of the voltage and current, the equivalent distributed circuit parameters of the multiconductor lines can be extracted.

When the frequency becomes higher, some wave properties such as radiation and surface wave appear. Only the guided-wave propagating along the lines is no longer correct. The effective loss due to radiation and coupling with surface-wave modes appears seriously, although the loss in conductors and dielectric media is being neglected. These are shown in the distributed impedance $Z = R + j\omega L$ and admittance $Y = G + j\omega C$. When the above effects do not appear, the impedance Z and admittance Y should only have imaginary part which means L and C are real values. When the frequency becomes higher, they become complex values. The real part of Z or Y represents the effective loss described above. For example, for the structure showed in Fig. 5 but, with parameters as $\varepsilon_r = 9.8, W = S = 1$ mm, $H = 0.635$ mm, the cutoff frequency of single line for lowest mode of TE-type surface wave is

$$f_c = \frac{c}{4H\sqrt{\varepsilon_r - 1}}. \tag{30}$$

The lowest mode of TM-type surface wave has no cutoff frequency, but at frequency

$$f = \frac{c \cdot tg^{-1}(\varepsilon_r)}{\sqrt{2}\pi H\sqrt{\varepsilon_r - 1}} \tag{31}$$

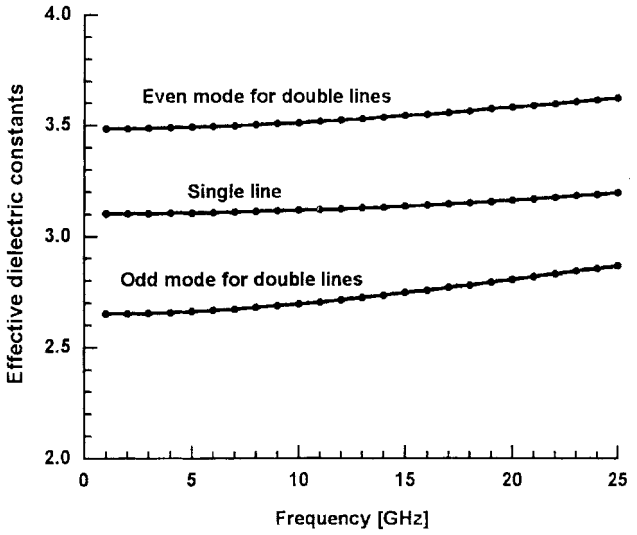

Fig. 8. Comparison of the effective dielectric constant parameters before (dash line with centered symbols) and after (solid line) voltage transformation.

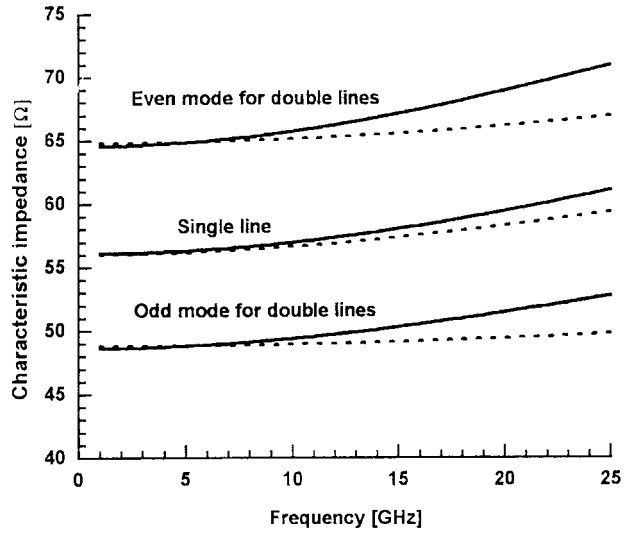

Fig. 9. Comparison of the characteristic impedance parameters before (dash line) and after (solid line) voltage transformation.

the TM-type surface wave couples with TEM main mode strongly [17].

With above geometrical parameters of the structure, one has $f_c = 39.8$ GHz and $f = 52.6$ GHz, respectively. Fig. 11 shows the ratio of R_{11} to ωL_{11} of $Z_{11} = R_{11} + j\omega L_{11}$ extracted by this method. The results show that when frequency is higher than 39 GHz, the ratio becomes larger which means the surface wave becomes stronger. When the frequency is close to $f = 52.6$ GHz, there is a very sharp change, which shows the coupling between TM-type surface wave and TEM main mode. In this case, the traditional distributed circuit parameters or descriptions are not suitable to this situation.

All this shows that the traditional equivalent circuit modeling with or without frequency-dependent parameters is valid when the radiation effects and coupling with surface wave are not yet strong. When these conditions are not satisfied, the system becomes very complicated, so it is impossible to be represented by a guided-wave system of the multiconductor lines. In that way, the parameter extraction is unlikely then.

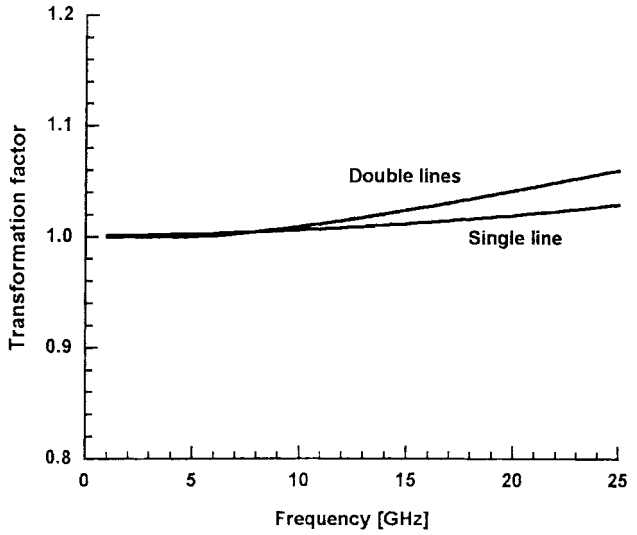

Fig. 10. The transformation factor as a function of the frequency.

VII. Conclusion

In this paper, a time-domain method for the extraction of frequency-dependent equivalent circuit parameters of multiconductor interconnection lines is presented. The reliability of the method is also illustrated. The frequency-dependent circuit parameters can be inserted into circuit-simulation software to investigate the time-domain response of high-speed IC systems, including multiconductor interconnections in VLSI. Those parameters can also be used in design microwave passive components in MIC. The problem of electromagnetic modeling of microwave structures has been discussed. The transformation between different $[L]$ and $[C]$ which, extracted from different defined voltage and current waveforms based upon introducing the voltage transformation factors, is also proposed. At the end of this paper, the application range of traditional distributed circuit modeling was discussed by numerical examples.

Appendix

From (2) and (9), one has

$$\frac{d}{dz}\begin{bmatrix} V_1 \\ V_2 \\ \vdots \\ V_N \end{bmatrix} = [e_{ij}]\,\mathrm{diag}\,(-\gamma_m)\,\mathrm{diag}\,(e^{-\gamma_m z})\begin{bmatrix} a_1 \\ a_2 \\ \vdots \\ a_N \end{bmatrix}$$

$$= -j\omega[L(\omega)][e_{ij}]\,\mathrm{diag}\left(\frac{1}{Z_{0m}}\right)\mathrm{diag}\,(e^{-\gamma_m z}) \cdot \begin{bmatrix} a_1 \\ a_2 \\ \vdots \\ a_N \end{bmatrix} \qquad (m = 1 \cdots N) \tag{A.1}$$

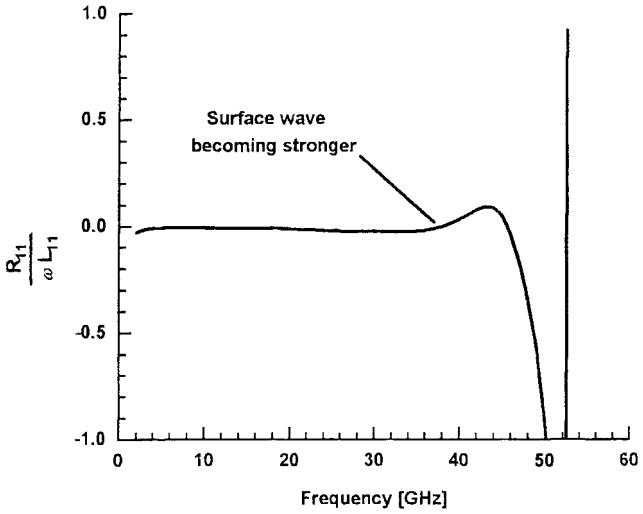

(a)

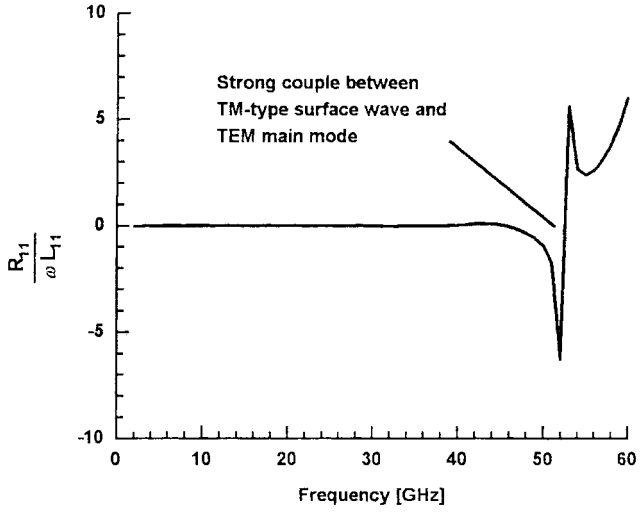

(b)

Fig. 11. The ratio of R_{11} to ωL_{11} of $Z_{11} = R_{11} + j\omega L_{11}$ extracted by this method for symmetric coupled transmission lines (see Fig. 5) with parameters: $\varepsilon_r = 9.8, W = S = 1$ mm, $H = 0.635$ mm. (a) Surface wave becoming stronger near $f = 38$ GHz. (b) Strong couple between TM-type surface with TEM main mode near $f = 53$ GHz. [(a) is enlarged from (b)].

and

$$\frac{d}{dz}\begin{bmatrix} I_1 \\ I_2 \\ \vdots \\ I_N \end{bmatrix} = [e_{ij}]\,\mathrm{diag}\left(\frac{1}{Z_{0m}}\right)\mathrm{diag}\,(-\gamma_m)\,\mathrm{diag}\,(e^{-\gamma_m z}) \cdot \begin{bmatrix} a_1 \\ a_2 \\ \vdots \\ a_N \end{bmatrix}$$

$$= -j\omega[C(\omega)][e_{ij}]\,\mathrm{diag}\,(e^{-\gamma_m z})\begin{bmatrix} a_1 \\ a_2 \\ \vdots \\ a_N \end{bmatrix} \quad (m = 1 \cdots N), \tag{A.2}$$

So $[L(\omega)]$ and $[C(\omega)]$ are

$$j\omega[L(\omega)] = [e_{ij}]\,\mathrm{diag}\,(\gamma_m)\,\mathrm{diag}\,(Z_{0m}[e_{ij}],^{-1} \quad (m = 1, \cdots, N) \tag{A.3}$$

and

$$j\omega[C(\omega)] = [e_{ij}]\,\mathrm{diag}\left(\frac{1}{Z_{0m}}\right)\mathrm{diag}\,(\gamma_m)[e_{ij}]^{-1}, \quad (m = 1, \cdots, N). \tag{A.4}$$

From (A.3) and (A.4), one can obtain the propagation constants

$$(j\omega)^2[L(\omega)][C(\omega)] = (j\omega)^2[C(\omega)][L(\omega)] = [e_{ij}]\,\mathrm{diag}\,(\gamma_m^2)[e_{ij}]^{-1}, \quad (m = 1, \cdots, N) \tag{A.5}$$

and the characteristic impedances

$$\mathrm{diag}\,(Z_{0m}) = j\omega[e_{ij}]^{-1}[L(\omega)][e_{ij}]\,\mathrm{diag}\left(\frac{1}{\gamma_m}\right), \quad (m = 1, \cdots, N). \tag{A.6}$$

The unique eigenmode matrix $[e_{ij}]$ can be obtained from taking orthogonal transformation on $j\omega[L(\omega)]$.

So, from the capacitance $[C]$ and inductance $[L]$ parameters we can obtain the propagation constants and characteristic impedances, and the whole procedure is very clear and simple.

The N-times orthogonal excitations guarantee that the voltage function matrix $[[V(z,\omega)]]$ and current function matrix $[[I(z,\omega)]]$ is nonsingular.

From (9), (12), and (13) one can see that after the N-times orthogonal excitations, the current function matrix $[[I]]$ in (9) at $z = 0$ becomes

$$\left[\begin{bmatrix} I_1(0) \\ 0 \\ \vdots \\ 0 \end{bmatrix}_1 \begin{bmatrix} 0 \\ I_2(0) \\ \vdots \\ 0 \end{bmatrix}_2 \cdots \begin{bmatrix} 0 \\ 0 \\ \vdots \\ I_N(0) \end{bmatrix}_N\right] = [e_{ij}]\,\mathrm{diag}\left(\frac{1}{Z_{0m}}\right)[[A]], \quad (m = 1, \cdots, N) \tag{A.7}$$

where

$$[[A]] = [e_{ij}]^{-1}\left[\begin{bmatrix} V_1(0) \\ V_2(0) \\ \vdots \\ V_N(0) \end{bmatrix}_1 \begin{bmatrix} V_1(0) \\ V_2(0) \\ \vdots \\ V_N(0) \end{bmatrix}_2 \cdots \begin{bmatrix} V_1(0) \\ V_2(0) \\ \vdots \\ V_N(0) \end{bmatrix}_N\right]. \tag{A.8}$$

So, from (4), (9), and (A.8) the voltage function matrix $[[V(z,\omega)]]$ and current function matrix $[[I(z,\omega)]]$ are

$$[[V(z,\omega)]] = [e_{ij}]\,\mathrm{diag}\,(e^{-\gamma_m z)}[[A]]$$

$$[[I(z,\omega)]] = [e_{ij}]\,\mathrm{diag}\left(\frac{1}{Z_{0m}}\right)\mathrm{diag}\,(e^{-\gamma_m z})[[A]], \quad (m = 1, \cdots, N). \tag{A.9}$$

From (A.7) and (A.8), one can see that the inverse matrix of $[[A]]$ and $[[V]]$ $(z = 0)$ exists. So, from equation (A.9), the

inverse matrix of $[[I]]$ and $[[V]]$ at z exists. This guarantees that (5) can be processed.

The numerical error analysis is briefly as follows. Because the derivation with respect to z is centrally different, so (A.9) becomes

$$\frac{d}{dz}[[V]] \approx [e_{ij}]\,\mathrm{diag}\,(-\gamma_m)\,\mathrm{diag}\,(e^{-\gamma_m z})[[A]] + \frac{1}{3!}[e_{ij}]\,\mathrm{diag}\,(-\gamma_m^3)\,\mathrm{diag}\,(e^{-\gamma_m z})[[A]]\,(dz)^2, \quad (m=1,\cdots,N) \tag{A.10}$$

and

$$[[I(z,\omega)]]^{-1} = [[A]]^{-1}\,\mathrm{diag}\,(e^{\gamma_m z})\,\mathrm{diag}\,(Z_{0m})[e_{ij}]^{-1}, \quad (m=1,\cdots,N). \tag{A.11}$$

From (A.10) and (A.11), $\Delta[Z]$ is

$$\Delta[Z] = \Delta j\omega[L(\omega)] = \frac{1}{3!}[e_{ij}]\,\mathrm{diag}\,(\gamma_m^3)\,\mathrm{diag}\,(Z_{0m})[e_{ij}]^{-1}\,(dz)^2, \quad (m=1,\cdots,N). \tag{A.12}$$

With the same procedure, $\Delta[Y]$ can be obtained

$$\Delta[Y] = \Delta j\omega[C(\omega)] = \frac{1}{3!}[e_{ij}]\,\mathrm{diag}\left(\frac{1}{Z_{0m}}\right)\mathrm{diag}\,(\gamma_m^3)[e_{ij}]^{-1}\,(dz)^2, \quad (m=1,\cdots,N). \tag{A.13}$$

ACKNOWLEDGMENT

The authors would like to thank Dr. J.-F. Mao and Prof. B.-H. Li for their helpful discussions on this paper.

REFERENCES

[1] C. Wei, R. F. Harrington, J. R. Mautz, and T. K. Sarkar, "Multiconductor transmission lines in multilayered dielectric media," *IEEE Trans. Microwave Theory Tech.*, vol. 32, pp. 439–449, Apr. 1984.

[2] H. Diestel, "Analysis of planar multiconductor transmission line systems with the method of lines," *AEU*, vol. 41, no. 3, pp. 169–175, 1987.

[3] S. P. Luo and Z. F. Li, "An efficient method for computing the capacitance matrix of multiconductor interconnects in very high-speed integrated circuit systems," *IEEE Trans. Microwave Theory Tech.*, vol. 43, pp. 225-227, Jan. 1995.

[4] Y. Fukuoka, Q. Zhang, D. P. Neikirk, and T. Itoh, "Analysis of multilayer interconnection lines for a high-speed digital integrated circuit," *IEEE Trans. Microwave Theory Tech.*, vol. 33, pp. 527–532, June 1985.

[5] F. Olyslager, D. D. Zutter, and K. Blomme, "Rigorous analysis of the propagation characteristics of general lossless and lossy multiconductor transmission lines in multilayered media," *IEEE Trans. Microwave Theory Tech.*, vol. 41, pp. 79–88, Jan. 1993.

[6] T. Dhaene and D. D. Zutter, "CAD-oriented general circuit description of uniform coupled lossy dispersive waveguide structures," *IEEE Trans. Microwave Theory Tech.*, vol. 40, pp. 1545–1554, July 1992 (Special Issue on Process-Oriented Microwave CAD Modeling).

[7] T. Dhaene, S. Criel, and D. D. Zutter, "Analysis and modeling of coupled dispersive interconnection lines," *IEEE Trans. Microwave Theory Tech.*, vol. 40, pp. 2103–2105, Nov. 1992.

[8] R. Mittra, W. D. Becker, and P. H. Harms, "A general purpose Maxwell solver for the extraction of equivalent circuits of electronic package components for circuit simulation," *IEEE Trans. Circuits Syst. I*, vol. 39, pp. 964–973, Nov. 1992.

[9] J. G. Yook, N. I. Dib, and L. P. B. Katehi, "Characterization of high-frequency interconnects using finite-difference time-domain and finite-element methods," *IEEE Trans. Microwave Theory Tech.*, vol. 42, pp. 1727–1736, Sept. 1994.

[10] K. S. Yee, "Numerical solution of initial boundary value problems involving Maxwell's equations in isotropic media," *IEEE Trans. Antennas Propagat.*, vol. AP-14, pp. 302–307, May 1966.

[11] D. M. Sheen, S. M. Ali, M. D. Abouzahra, and J. A. Kong, "Application of the three-dimensional finite-difference time-domain method to the analysis of planar microstrip circuits," *IEEE Trans. Microwave Theory Tech.*, vol. 38, pp. 849–857, July 1990.

[12] J. Fang, "Electromagnetic modeling of electronics packaging by the time-domain finite-difference method," in *Proc. IEEE Topical Meet. Elect. Performance Electron. Packaging*, 1992, pp. 90–92.

[13] M. P. May, A. Taflove, and J. Baron, "FDTD modeling of digital signal propagation in 3-D circuits with passive and active loads," *IEEE Trans. Microwave Theory Tech.*, vol. 42, pp. 1514–1523, Aug. 1994.

[14] R. E. Collin, *Fiele Theory of Guided Waves*. New York: McGraw-Hill, 1960.

[15] K. K. Mei and J. Y. Fang, "Superabsorption—A method to improve absorbing boundary conditions," *IEEE Trans. Antennas Propagat.*, pp. 1001–1010, Sept. 1992.

[16] J. R. Brews, "Characteristic impedance of microstrip lines," *IEEE Trans. Microwave Theory Tech.*, vol. MTT-35, pp. 30–33, Jan. 1987.

[17] T. C. Edwards, *Foundations for Microstrip Circuit Design*. New York: Wiley, 1981.

Jin Zhao was born in Liaoning, China, in 1968. He received the B.S. degree from the Beijing Institute of Technology, China, in 1991, and the M.S. and Ph.D. degrees from Shanghai Jiao Tong University, China, in 1993 and 1996, all in electromagnetic field theory and microwave technology.

From September 1996, he worked as Post-Doctorate Associate at the Department of Department of Electrical Engineering, State University of New York at Binghamton. His research interests include computational electromagnetism, transmission line theory, electrical performance of electronics packaging, microwave and millimeter-wave integrated circuits and components, and microwave antennas.

Zheng-Fan Li graduated from the Department of Radioelectronic Engineering, Tsinghua University, Beijing, China, in 1958.

Beginning in 1958, he worked at Tsinghua University for 21 years, first as an Assistant, then as a Lecturer, and finally, as an Associate Professor. In 1979, he transferred to Jiao Tong University, Shanghai, China. He was with the Department of Electrical Engineering, Cornell University, Ithaca, NY, as a Foreign Visiting Scholar from 1981 to 1983. He is now with the Department of Electronic Engineering, Jiao Tong University, as a Professor. He is an Editor of the *Journal of China Institute of Communication and Journal of Microwaves*. He has performed research in the fields of electromagnetic field theory, radar systems, microwave integrated circuits, and microwave FET linear and nonlinear circuits. Recently, his interests include analysis of high-speed IC systems and packaging structures, including extraction of the circuit parameters with electromagnetic field methods, and circuit simulation of the high-speed IC systems.

Dr. Li is a committee member of the Microwave Communication Society of China.